Supplementary Information for:

Merging gold plasmonic nanoparticles and L-proline inside MOF for plasmon-induced visible light chiral organocatalysis at low temperature

A. Kushnarenko[a], A. Zabelina[a], O. Guselnikova[a,b], E. Miliutina[a], B. Vokatá[a], D. Zabelin[a], V. Burtsev[a] , R. Valiev[c], Z. Kolska[d], M. Paidar[e], V. Sykora[f], P. Postnikov[a,b*], V. Svorcik[a], O. Lyutakov[a*]

[a] *Department of Solid State Engineering, University of Chemistry and Technology, 16628 Prague, Czech Republic*

[b] *Research School of Chemistry and Applied Biomedical Sciences, Tomsk Polytechnic University, Russian Federation*

[c] *Kazan Federal University, 420008 Kazan, Russian Federation*

[d] *Centre for Nanomaterials and Biotechnology, J. E. Purkyne University, 40096 Usti nad Labem, Czech Republic*

[e] *Department of Inorganic Technology, University of Chemistry and Technology, 16628 Prague, Czech Republic*

[f] *Department of Water Technology and Environmental Engineering, University of Chemistry and Technology, 166 28 Prague, Czech Republic*

---

* *Corresponding authors: postnikov@tpu.ru, lyutakoo@vscht.cz*

Experimental

Materials

Zirconium (IV) chloride, 2-aminoterephthalic acid (99 %), acetic acid (100 %), dinethyl formamide, ethanol ((>96 %), deionized water (DI), gold(III) chloride hydrate (99,99 %), silver nitrate (99,99 %), trisodium citrate dihydrate (99,99 %, Supelco), sodium borohydride (99 %), hydrochloric acid (35 %, ACS reagent), sodium hydroxide (≥98 %), 4-chlorbenzaldehyde (97 %), 4-nitrobenzaldehyde (≥98 %), L-proline (≥99 %), hexane (≥99 %), ethyl acetate (≥99,7 %), 2,2,6,6-Tetramethylpiperidine 1-oxyl (TEMPO), 2-Butanone, Behzaldehyde, methanol (reagent grade, ≥ 99%) were purchased from Sigma-Aldrich. Silica (pore size 60 Å, particle size 230-400 mesh) was purchased from Supelco.

Samples preparation

***Preparation of AuNPs**:* Gold nanoparticles were prepared using the Turkevich method [[1]]. Firstly, 2.15 mL of a 0.03 M $HAuCl_4$ solution (25 mL) was rapidly added to 215 mL of refluxed water under continuously stirring. Next, 5.4 mL of a 0.04 M trisodium citrate solution (25 mL) was added drop-wise to the resulted solution. After cooling, the AuNPs were separated by centrifugation and washed several times using 15 mL of DI water with sonication and separation cycles. Subsequently, the AuNPs were dispersed in DMF before UiO-66-NH_2 synthesis.

Preparation of AgNPs: Silver nanoparticles were synthesized using the following method: ice-cold sodium borohydride solution (30 mL, 0.02 M) was added to a flask placed in an ice bath and stirred for 30 min. Next, 2 mL of 0.01 M solution of $AgNO_3$ was added dropwise. Stirring was stopped as soon as all of the $AgNO_3$ was added. The formation of AgNPs was monitored by the color change of the solution from colorless to dark yellow. Subsequently, the AgNPs were isolated by centrifugation and re-dispersed in DMF before UiO-66-NH_2 synthesis.

***Preparation of UIO-66-NH_2**:* Zirconium (IV) chloride (0.6 mmol), 2-aminoterephthalic acid (0.6 mmol), and acetic acid (2 mL) were dissolved in 15 mL of DMF. The solution was sonicated for 30 minutes and then transferred to a 25 mL teflon-lined autoclave. The temperature was maintained at 120 °C for 24 hours. Finally, a dark blue powder was obtained, which was washed with DMF and ethanol (3 x 10 mL). The powder was additionally immersed in ethanol for 3 days, decanted and dried at 80 °C under vacuum for 24 hours [[2]].

***Preparation of Me@UIO-66-NH_2**:* Preparation of both Au@UIO-66-NH_2 and Ag@UIO-66-NH_2 was provided with the same method, with adding of various amounts of AuNPs or AgNPs (by their ultrasound-assisted dispersion) in UiO-66-NH_2 reaction mixture before solvothermal synthesis.

Proline entrapping and Me@UIO-66-NH_2/proline preparation: 5 g of Me@UIO-66-NH_2 (or UIO-66-NH_2 in the control experiments) were added to 10 mL of proline solution (0.5 mM) in acetone and gently stirred for 3 hours. The Me@UIO-66-NH_2 powders with entrapped proline molecules were separated by centrifugation and dried under vacuum. The entrapping of proline molecules was confirmed by total organic carbon (TOC) content analysis in supernatant after evaporation, drying and redissolving in Milli-Q water. The procedure was repeated two times for the pristine proline solution, proline solution after its interaction with Me@UIO-66-NH_2 powders, and Me@UIO-66-NH_2 powders dispersed in acetone without proline addition.

Racemic aldol reaction: To the solution of 4-nitrobenzaldehyde (0.5 g, 3.3 mmol) in acetone (6 mL) was added 1 % (w/v) NaOH solution at 0 °C. The reaction mixture has been strirred during 15 min at 0 °C. The resulted solution was neutralized (pH - 6) by adding 0.5 N HCl solution and dried under vacuum. After, the yellow powder was redisperged in 12.5 mL of H_2O and extracted by EtOAc (3 x 30 mL). After evaporation the residue was purified by flash chromatography (silica,

EtOAc:hexane = 80:20) providing 580 mg of 4-hydroxy-4-(4-nitrophenyl)butan-2-one as a yellow oil [3]. NMR spectra of resulted product were identical to previously reported [4]. The racemic 4-hydroxy-4-(4-nitrophenyl)butan-2-one has been used as a standard for the GC determination of yield and enantiomeric excess.

The structure and purity of the reaction products analyzed by GC-MS. GC: Agilent 7890B (Agilent Technologies), Rxi-5ms column (20 m x 0.18 mm, RESTEK), carrier gas: He 6.0; flow rate: 0.7 mL/min. MS: Agilent 7010 QQQ (Agilent Technologies), EI + 70 eV ionization, scan rate: 4 scans/s.

^{1}H NMR and MS data for products:

4-(4-Chlorophenyl)-4-hydroxybutan-2-one: ^{1}H NMR (400 MHz, $CDCl_3$): δ 7.35 (m, 4H), 5.16 (m, 1H), 3.42 (d, 1H), 2.80 (m, 2H), 2.22 (s, 3H). MS (EI): m/z 200, 197.91, 182.04, 180.03, 164.89, 145.02, 142.24, 139.23, 111.01, 77. MS (EI): m/z 180, 165, 137, 101.9, 74.8, 50.98, 42.9.

4-hydroxy-4-(4-nitrophenyl)butan-2-one: ^{1}H NMR (400 MHz, $CDCl_3$) δ 8.17 (d, 2H), 7.6 (d, 2H), 5.29 (m, 1H), 3.56 (s, 1H), 2.83 (m, 2H), 2.18 (s, 3H). MS (EI): m/z 208.86, 190.88, 173.92, 150.86, 105, 103.08, 76.84, 58, 50.75, 42.91.

Plasmon-assisted enantioselective aldol reaction using Me@UiO-66-NH$_2$/proline. 26 mg of Me@UIO-66-NH_2/proline powder was dispersed in a solution of 4-chlorobenzaldehyde or 4-nitrobenzaldehyde (0.1 mmol, 2 mL acetone, 0.5 mL chloroform). Aldol reactions were carried out at -20 °C under illumination with an LED light source (550 nm central emission wavelength, Thorlabs, irradiance on the first glass surface – 100 mW/cm^2). In control experiments, reactions were carried out in the dark and/or at RT.

The final solution was centrifuged, and 1 mL was taken to use in GC-MS to determine the conversion of the reactant and yield.

The reaction conversion, yield, and enantiomeric excess were also determined by GC, using a capillary chiral column (β-DEX ™ 120 chiral capillary column, L × I.D. 30×0.25 mm^2, df 0.25 μm, Supelco) using racemic 4-hydroxy-4-(4-nitrophenyl)butan-2-one as a standart.

To calculate the conversion, the calibration curve was prepared using 5 solutions with different concentration of reactants (40, 20, 10, 5 and 2.5 mM). The enantiomeric excess was determined from the ratio of enantiomer peak intensities using equation:

$$\%\, ee = \frac{((R) - (S))}{((R) + (S))} * 100\ \%$$

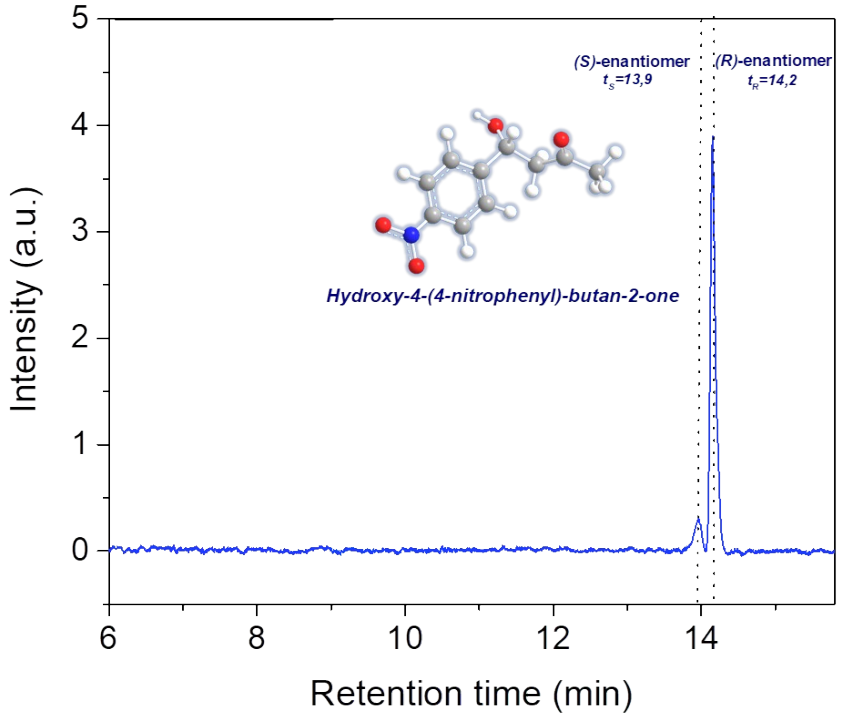

Gas chromatogram of 4-hydroxy-4-(4-nitrophenyl)butan-2-one

Control experiment with UiO-66-NH_2/proline (absence of AuNPs). 25 mg of UIO-66-NH_2/proline (proline loading ca 2.5 mM) powder was dispersed in a solution of 4-nitrobenzaldehyde (0.1 mmol, 2 mL acetone, 0.5 mL chloroform). Aldol reaction was carried out at -20 °C under illumination with an LED light source (550 nm central emission wavelength, Thorlabs, irradiance on the first glass surface – 100 mW/cm^2). The final solution was centrifuged, and 1 mL was taken to use in GC-MS to determine the reaction conversion.

Control experiment with AuNPs/proline (without UiO-66-NH_2, i.e. absence of spatial proximity of AuNPs and proline ensured). AuNPs (ca 0.3 mg) were dispersed in the mixture of acetone and chloroform (0.1 mmol, 2 mL acetone, 0.5 mL chloroform). Then proline (2.5 mM) and 4-nitrobenzaldehyde were added. Aldol reaction was carried out at -20 °C under illumination with an LED light source (550 nm central emission wavelength, Thorlabs, irradiance on the first glass surface – 100 mW/cm^2). The final solution was centrifuged, and 1 mL was taken to use in GC-MS to determine the reaction conversion.

Control experiment with AuNPs@UiO-66-NH_2 (absence of proline). 25 mg of Au@UIO-66-NH_2 powder was dispersed in a solution of 4-nitrobenzaldehyde (0.1 mmol, 2 mL acetone, 0.5 mL chloroform). Aldol reaction was carried out at -20 °C under illumination with an LED light source

(550 nm central emission wavelength, Thorlabs, irradiance on the first glass surface – 100 mW/cm^2). The final solution was centrifuged, and 1 mL was taken to use in GC-MS to determine the reaction conversion.

Control experiment with benzaldehyde and 2-butanon A suspension was prepared by dispersing 30 mg of Au@UIO-66-NH_2/proline powder into a mixture containing benzaldehyde (0.1 mmol) dissolved in 2-butanone (2 mL) and chloroform (0.5 mL). The blend was stirred at -20 °C under simultaneous illumination by an LED with 550 nm wavelength for 48h (control reaction was performed without light illumination, also at at -20 °C). Then the Au@UIO-66-NH_2/proline powder was isolated through centrifugation, and the resulting mixture was analyzed by GC-MS.

GC curves were obtained using Agilent 7010 GC gas chromatograph with a flame ionization detector (FID) and a HP-5 column (30 m x 250 µm x 0.25 µm). GC program was: 50 °C (3 min) - > 10 °C/min - > 250 °C (10 min), carrier gas: Helium, constant flow 0.4 ml/min, spray: 1 µl, split 10:1, temperature 250 °C.

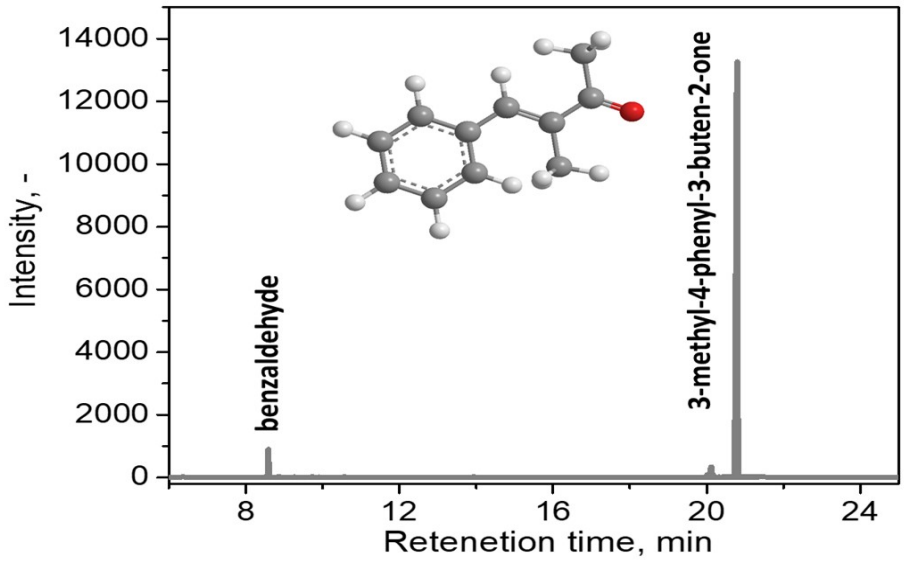

Gas chromatogram, measured after control experiment: Au@UiO-66-NH_2/proline catalysed reaction between benzaldehyde and 2-butanon (reaction was performed at -20 ^oC under illumination).

3-methyl-4-phenyl-3-buten-2-one: 1H NMR (400 MHz, CDCl3): δ 7.52 (q, 1H), 7.34 (m, 4H), 7.31 (m, 1H), 2.46 (s, 3H), 2.05 (d, 3H). 13C NMR (CDCl3, 100.6 MHz): δ 200.0, 139.6, 137.7, 136.0, 129.6, 128.6, 128.5, 25.8, 12.9.

Control experiment with $AgNO_3$ addition. 30 mg of Au@UIO-66-NH_2 powder was dispersed in a solution of $AgNO_3$ (0.011 mmol, 5 mL methanol) and mixed for 24 h at RT under 550 nm light irradiation and at the dark for a control. The resulting powder after experiments was washed 10 times

with water and 3 times with MeOH, dried under vacuum for 5 h and subjected to SEM-EDX analysis.

Control experiment with TEMPO. First suspension was prepared by dispersing 30 mg of Au@UIO-66-NH_2/proline powder into a mixture containing 4-nitrobenzaldehyde (0.1 mmol) dissolved in acetone (2 mL) and chloroform (0.5 mL). Then TEMPO (10^{-6} M or 10^{-4} M) was introduced into the solution. The reaction was conducted at -20 °C under illumination with LED at 550 nm wavelength. Following the reaction, the Au@UIO-66-NH_2/proline powder was isolated through centrifugation, and the resulting mixture was analyzed by GC-MS.

Measurement Techniques

Fourier transforms infrared (FT-IR) spectra were measured on Nicolet 6700 Spectrometer (Thermo Scientific, France) ATR. All measurements were performed in the spectral range from 629 to 4000 cm^{-1} at a resolution of 4 cm^{-1}.

The *XRD patters* were collected using PANalytical X'Pert PRO XRD-diffractometer with Cu Kα radiation (1.5406 Å) UiO-66-NH_2, UiO-66-NH_2@Au, proline, and UiO-66-NH_2@Au/proline.

Transmission electron microscopy (TEM) images were obtained with JOEL JEM-1010 instrument (Japan).

SEM images were obtained using on Lyra3 GMU (Tescan, CR) microscope with 2 kV accelerating voltage. *EDX* mapping was performed with utillization of X-MaxN EDX analyzer.

UV-Vis absorption spectra were measured by Lambda 25 UV-Vis/NIR Spectrometer (PerkinElmer, USA) at a scanning rate of 480 nm/min.

Surface area and porosity of UIO-66-NH_2, UIO-66-NH_2@Au and UIO-66-NH_2@Au/proline powders were determined using N_2 (99.999 %, Linde Gas) adsorption/desorption isotherms (NOVA3200, Anton Paar, Austria), quantified by NovaWin software (5 points of Brunauer-Emmett-Teller, BET model for surface area and DFT model for pore volume. Samples were measured 3x.

The *total organic carbon* content was established using a TOC-VCPH analyzer (Shimadzu, Japan), according to the standard ISO 8245 Water Quality.

The *X-ray photoelectron spectroscopy (XPS)* was performed using an Omicron Nanotechnology ESCAProbeP spectrometer fitted with a monochromated Al K Alpha X-ray source working at 1486.6 eV. The energy resolution was 0.4 eV for the study and 0.1 eV for measuring the high-resolution XPS spectra.

Zr and Au traces in reaction mixtures were determined by *inductive coupled plasma emission* spectrophotometer with optical detector (Optima 8000 ICP-OES, PerkinElmer, USA). Before measurements the reaction mixture(s) were evaporated, and residuals were dissolved in aqua regia.

Hybrid (photo)catalyst optimization

Considering the relatively high cost of plasmon-active metals compared to MOFs, the catalyst was optimized primarily by adjusting the type and amount of plasmon-active metals used. In initial experiments, we tested silver and gold nanoparticles as a potential plasmon-active cores. We prepared Au@UiO-66-NH_2 and Ag@UiO-66-NH_2 and subsequently loaded it by proline. Then, these materials were used in the model aldol reaction between acetone and 4-nitrobenzaldehyde (550 nm LED illumination, 72 hours). However, in the case of Ag@UiO-66-NH_2, we did not observe any traces of desired product, according to GC measurements. The dominant process was the oxidation of the benzaldehyde(s), catalyzed by Ag. As a result, we were forced to focus on gold nanoparticles and related Au@UiO-66-NH_2 (photo)catalysts.

The next optimization step involved testing of different amount of gold in the preparation of MOFs. Considering the nature of MOF formation, we used different amounts of AuNPs while maintaining a constant concentration of UiO-66-NH_2 precursors. We then measured the efficiency of the resulting (photo)catalyst in the model aldol reaction between acetone and nitrobenzaldehyde. The analytical yield of 4-hydroxy-4-(4-nitrophenyl)butan-2-one is shown in Fig. S1 as a function of Au@UiO-66-NH_2/proline composition. As Fig. S1 indicates, low concentrations of Au (i.e., small amounts of AuNPs in Au@UiO-66-NH_2/proline) did not provide sufficient amounts of 4-hydroxy-4-(4-nitrophenyl)butan-2-one. Gradually increasing the concentration of Au (and, correspondingly, the amount of AuNPs in the Au@UiO-66-NH_2 structure) resulted in a significant increase in the efficiency of the (photo)catalyst. The optimal concentration of Au was found to be approximately 100 mg/L. Further increases in the concentration of AuNPs did not improve efficiency, and we observed an efficiency saturation and even its decrease for concentrations of Au above 150 mg/L.

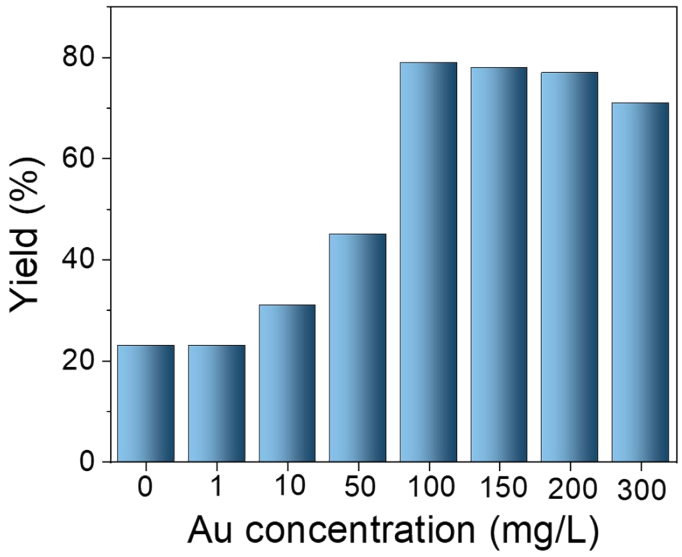

Fig. S1 Yield of 4-hydroxy-4-(4-nitrophenyl)butan-2-one as a function of Au concentration (addition of AuNPs before UiO-66-NH_2 solvothermal synthesis) during the preparation of Au@UiO-66-NH_2

Table S1.

XPS-measured element composition of UIO-66-NH_2 and Au@UIO-66-NH_2 (according to Fig. S3A).

Sample	**Elements (at. %)**				
	C	***O***	***N***	***Zr***	***Au***
UIO-66-NH$_2$	57,7	32,3	4,7	5,3	-
Au@UIO-66-NH$_2$	60,4	30,3	3,1	5,3	0,9

Affiliation of FTIR peaks (according to Fig. S3B):

3476, 3357 cm^{-1} – asymmetric and symmetric NH_2 vibrations;

1657, 1575 cm^{-1} – asymmetric and symmetric stretching of carboxyl groups;

1500 cm^{-1} – C=C stretching of benzene ring;

1435 cm^{-1} – C-C stretching;

1383 cm^{-1} – C-N stretching vibration of aromatic amines;

1256 cm^{-1} – C-O stretching;

1160 cm^{-1} – C-C stretching vibration;

766 cm^{-1} – C=C stretching vibration;

663 cm^{-1} – Zr-(OC) asymmetric stretching vibration.

Results of surface area and porosity determination

Table S2

N_2 adsorption-desorption data of UiO-66-NH_2, Au@UiO-66-NH_2, and Au@UiO-66-NH_2/proline powders.

Sample	**Surface area** (m^2/g)	**Pore volume** (cm^3/g)
UiO-66-NH$_2$	820.2±15.5	0.167±0.045
Au@UiO-66-NH$_2$	836.6±27.7	1.116±0.038
Au@UiO-66-NH$_2$proline	180.4±5.4	0.256±0.006

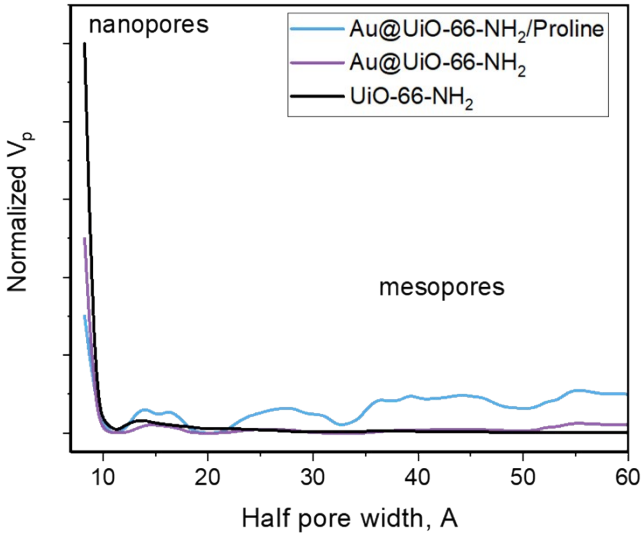

Fig. S2 Pore size distribution of UiO-66-NH_2, Au@UiO-66-NH_2, and Au@UiO-66-NH_2/proline

Fig. S2 and Table S2 – related discussion UiO-66-NH_2 shows typical surface area [5] with the dominant presence of nanopores. Further synthesis of UiO-66-NH_2 in the presence of AuNPs leads to a slight increase to 836 m^2/g in the surface area and increased pore volume, possibly due to the defective structure. The loading of proline to Au@UiO-66-NH_2 leads to the suppression of pore volume with the suppression of the relative amount of nanopores probably due to the blocking of pores by proline.

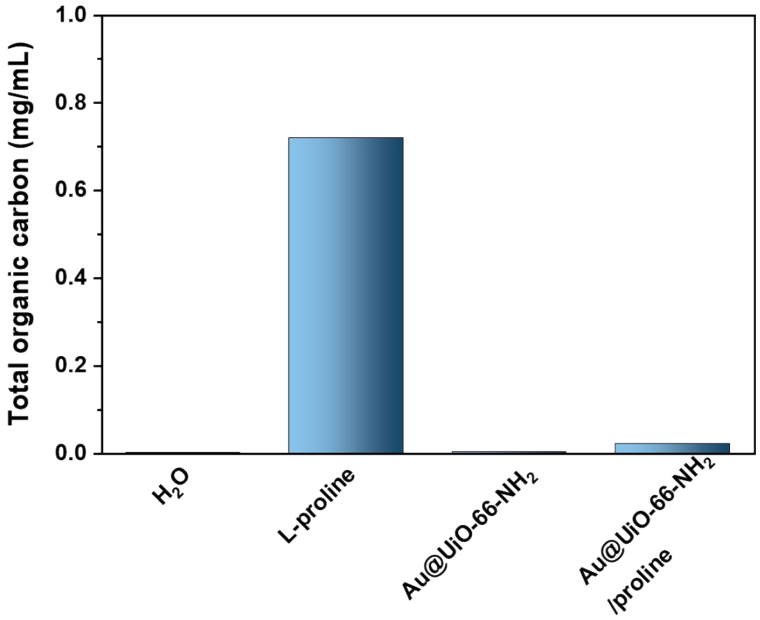

Fig. S3 Concentration of organic carbon in pristine water, proline solution, and supernatants of Au@UiO-66-NH_2 (after centrifugation) after its interaction with water or proline solution

Fig. S3 – related discussion. To confirm the ability of Au@UiO-66-NH_2 to capture proline, we conducted additional experiments. First, we dispersed 5 g of Au@UiO-66-NH_2 powder in a 10 mL solution of acetone and proline (0.5 mmol) under rigorous stirring for 3 hours. After, we removed the powder by centrifugation, dried the supernatant, and re-dissolved it in DI water. We measured the concentration of organic carbon before and after the interaction of proline with the Au@UiO-66-NH_2 powder, and the results are presented in Fig. S4. We noted that the pure water contained a negligible amount of organic carbon, which had no effect on the results. Dispersion of Au@UiO-66-NH_2 powder in pristine water (without proline) and subsequent centrifugation led to a slight increase in organic carbon content, but the effect was not pronounced. The concentration of organic carbon in the proline solution was found to be 0.7 mg/mL, as expected for the procedure we used (the acetone was completely removed, and the residue was re-dissolved in DI water). However, after interaction of the proline solution with Au@UiO-66-NH_2 powder and subsequently separating the Au@UiO-66-NH_2, a significant decrease in organic carbon was observed. This indicates that the proline was successfully entrapped in the MOF pores and removed from the solution by centrifugation together with Au@UiO-66-NH_2.

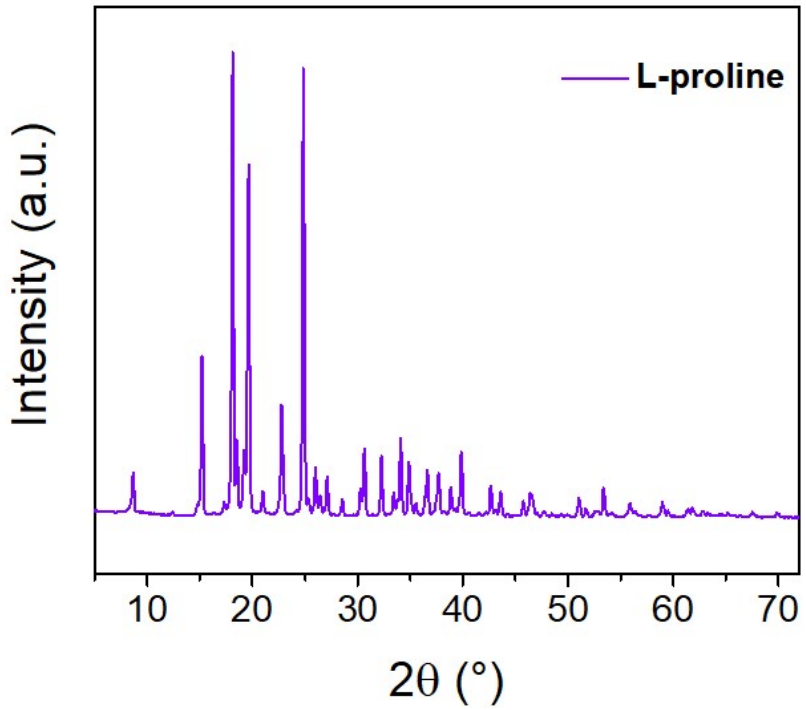

Fig. S4 XRD pattern of L-proline powder obtained after dissolution in DI and drop deposition/drying on glass substrate

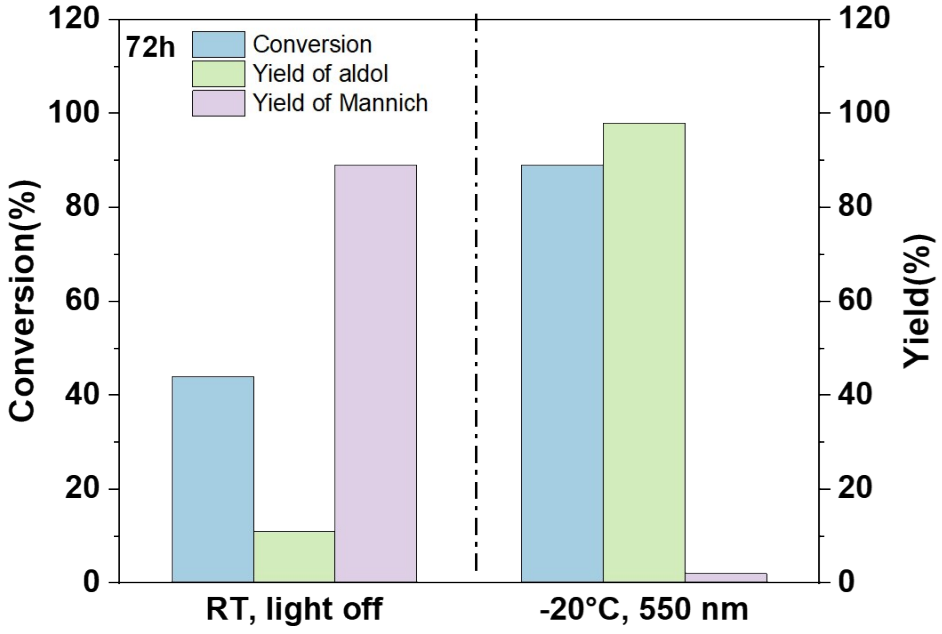

Fig. S5 Comparison of catalytic performance of Au@UiO-66-NH_2/proline in aldol reaction 4-chlorobenzaldehyde with acetone

Fig. S6 Plasmon-induced conversion of benzaldehyde at -20°C with or without light illumination (reaction proline between benzaldehyde and 2-butanon was catalysed by Au@UiO-66-NH_2/proline.

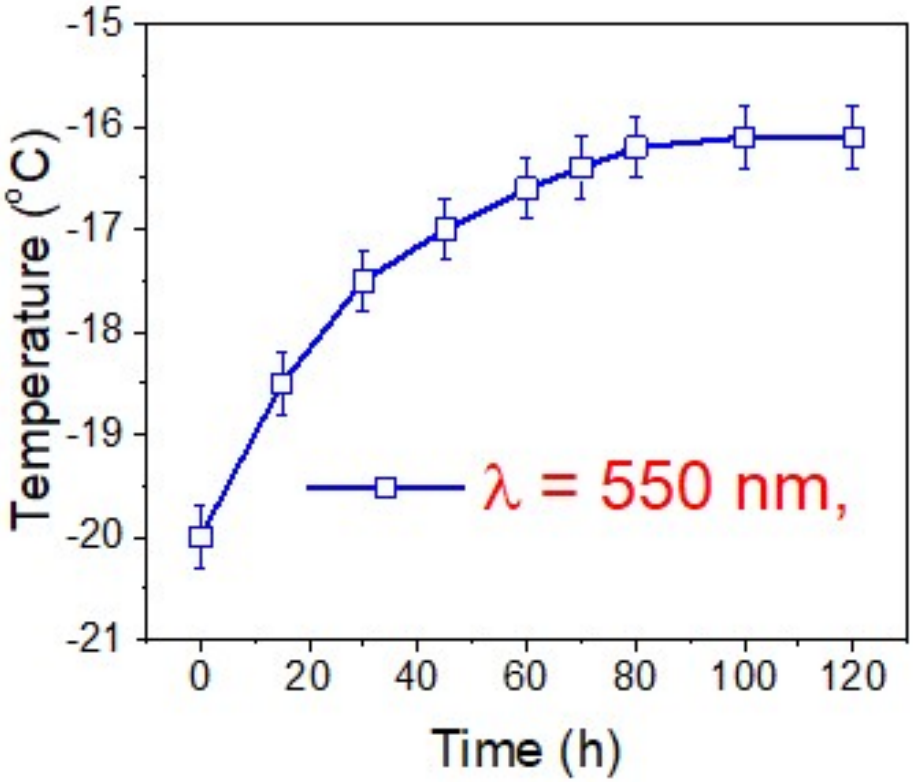

Fig. S7 Increase of reaction mixture temperature (from "starting" -20 °C) under illumination of Au@UiO-66/proline suspension (550 nm LED, irradiance on the first glass surface – 100 mW/cm^2)

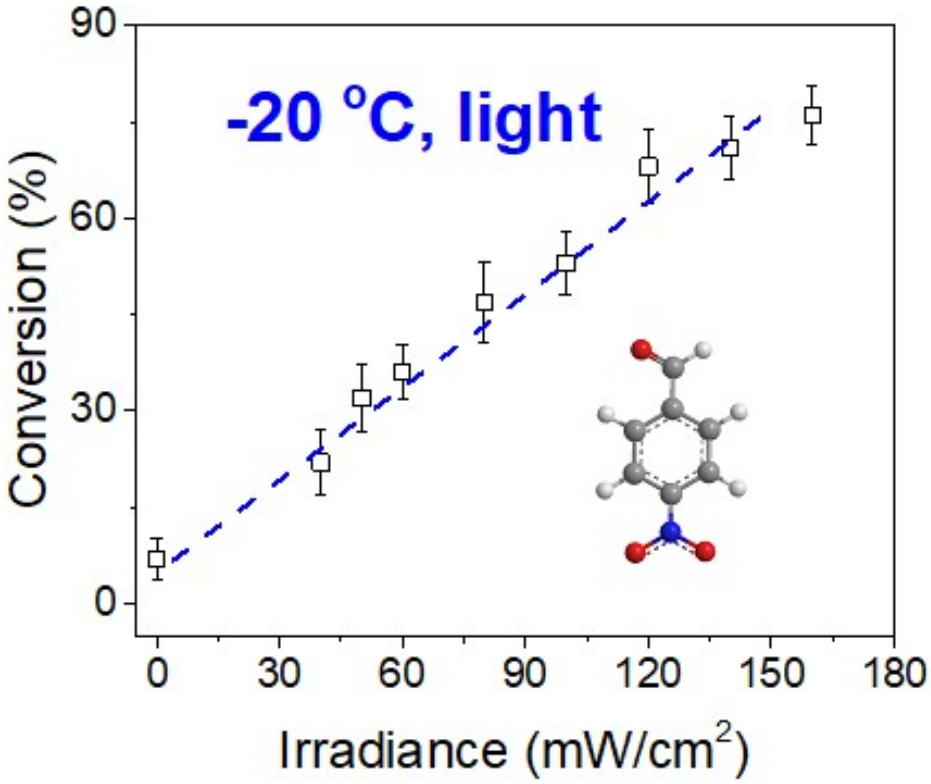

Fig. S8 4-nitrobenzaldehyde conversion as a function of LED irradiance (-20 °C, 36 h)

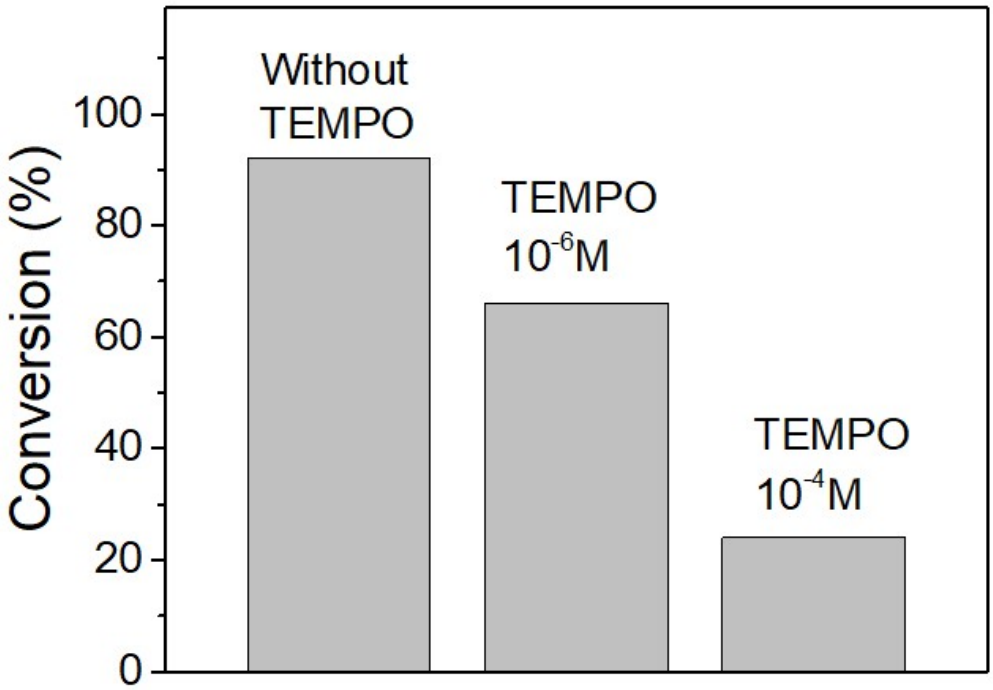

Fig. S9 Plasmon-induced conversion of 4-nitrobenzaldehyde in the presence or absence of TEMPO-scavengers.

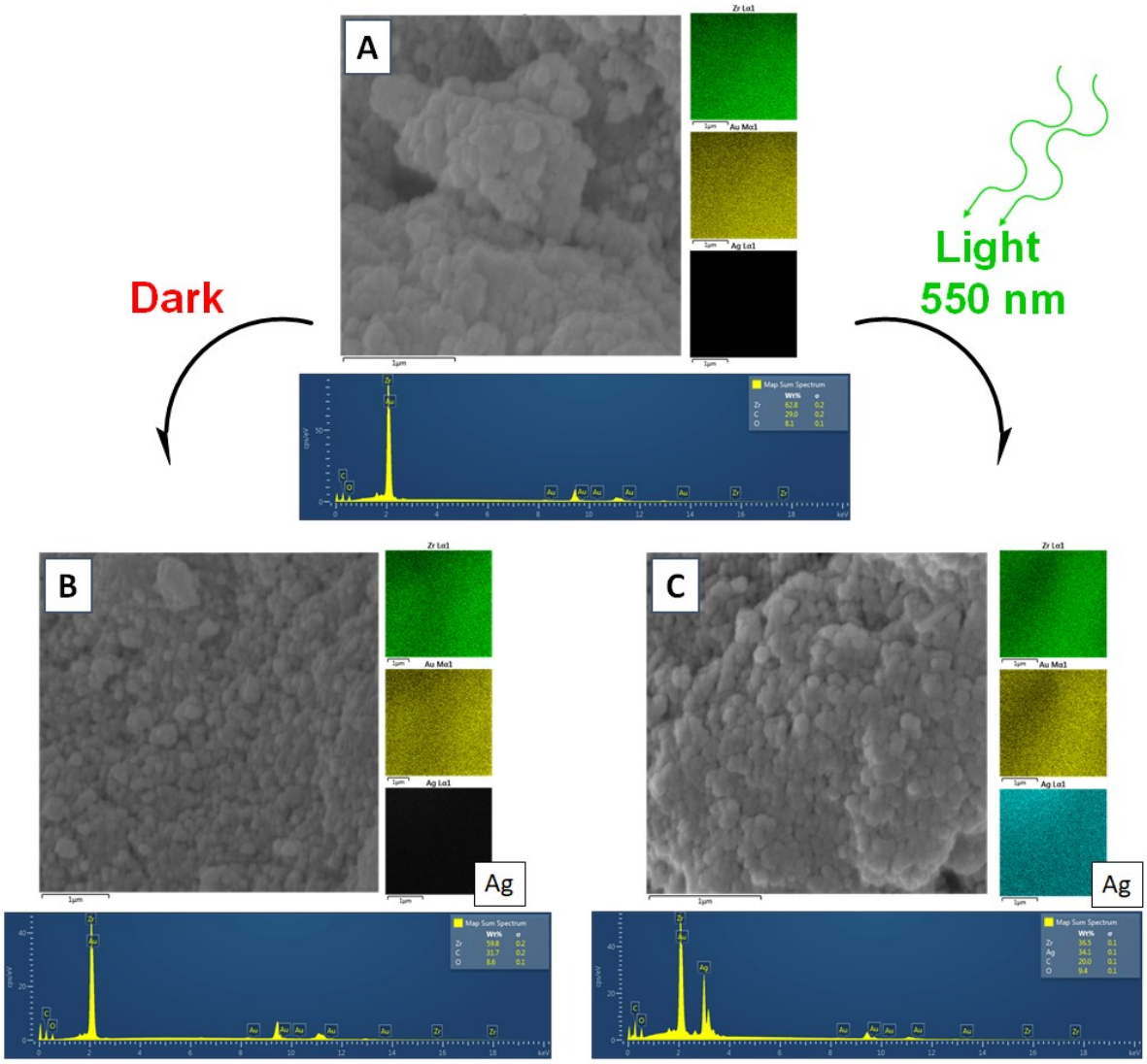

Fig. S10 SEM images with EDX mapping and EDX point analysis together with the results for the main elements: Zr, Au, C, O and Ag for Au@UiO-66-NH_2 (A) before the control experiment with $AgNO_3$ addition, (B) after an experiment in the dark and (C) under 550 nm light irradiation.

Table S3 Determined by EDX (Fig. S10) samples composition.

Au@UiO-66-NH_2/proline	Elemental concentrations (wt. %)			
	Zr	C	O	Ag
before	62.8	29.0	8.1	0.0
after (dark)	59.8	31.7	8.9	0.0
after (550 nm)	36.5	20.0	9.4	34.1

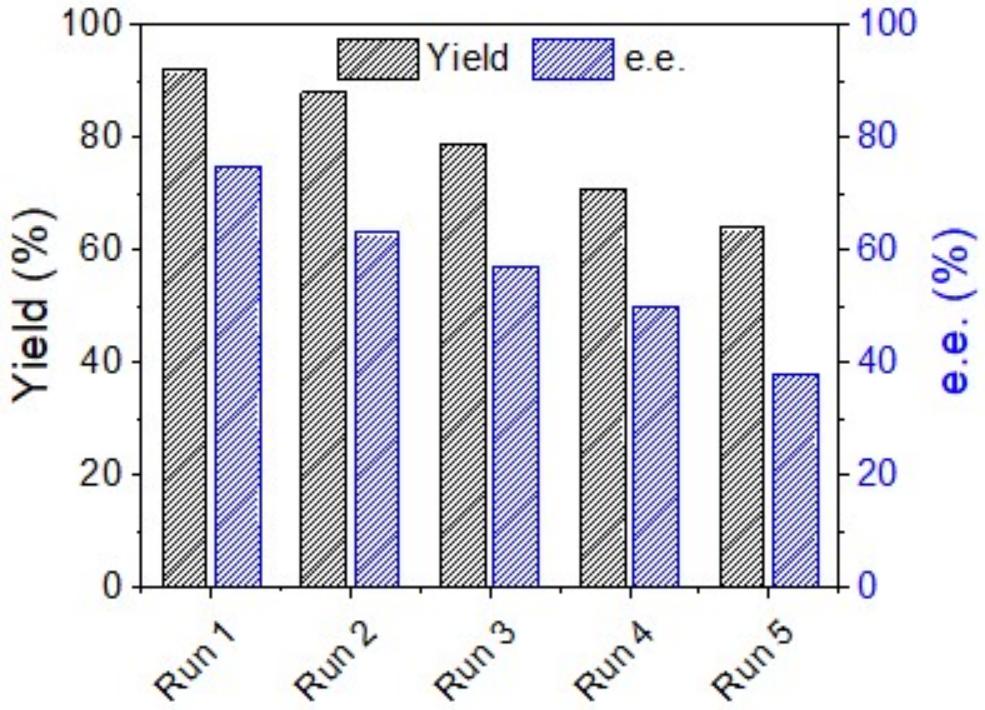

Fig. S11 (A) – yields and *ee* of 4-hydroxy-4-(4-nitrophenyl)butan-2-one in the several subsequent cycles of Au@UiO-66 utilization at RT (plasmon triggering, 24 h)

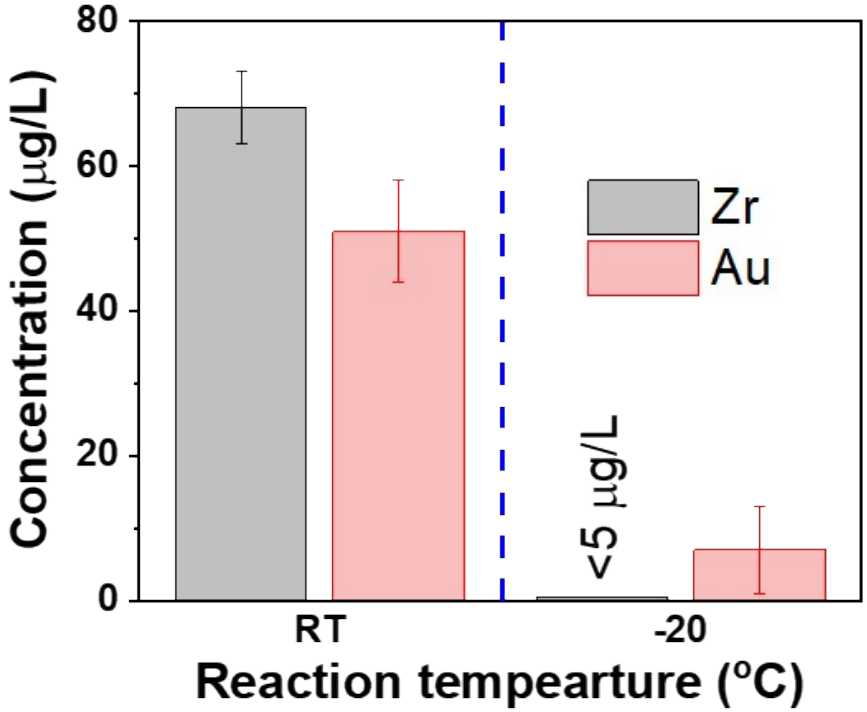

Fig. S12 ICP-OES measured concentrations of the trace amounts of residual Zr and Au in the reaction mixture as a function of reaction temperature (Au@UiO-66, light)

Density functional calculation of plasmon assisted reaction pathway(s).

Calculation details

The optimization of ground and first excited states of anion and dianion was carried out using the time dependent density functional theory [6] with B3LYP [7] functional and 6-31G(d,p) basis set in Turbomole software [8]. All calculations were done in "SKIF" supercomputer in Russia. The S_1 state has found to be decay and, due to this reason, the geometry has not been provided.

Geometries of molecules:

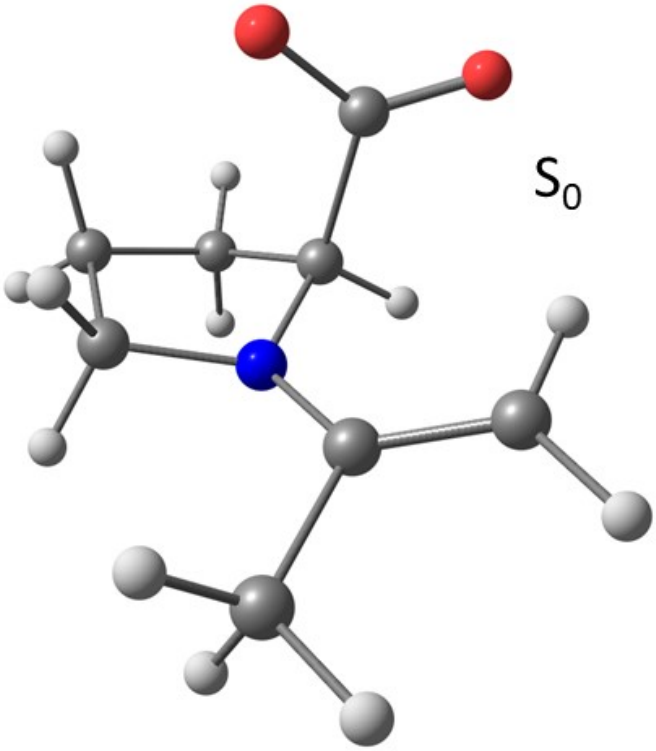

C	-1.836507000	-0.917952000	-0.338288000
C	-1.192593000	0.377771000	0.208520000
N	0.119338000	-0.041416000	0.709442000
C	0.482021000	-1.364202000	0.173370000
C	-0.896759000	-2.045277000	0.129635000
C	1.165059000	-1.329689000	-1.252309000
O	2.272050000	-1.914824000	-1.328578000
O	0.501466000	-0.734703000	-2.143506000
C	1.088993000	0.868775000	1.095777000
C	2.418811000	0.629937000	1.037175000
C	0.561969000	2.161438000	1.682665000
H	-2.869106000	-1.046550000	0.010777000
H	-1.815891000	-0.881867000	-1.427202000
H	-1.104352000	1.119022000	-0.597672000
H	-1.792257000	0.825074000	1.016800000
H	1.165708000	-1.851999000	0.877170000
H	-0.910788000	-2.906998000	-0.544801000

H	-1.178268000	-2.392228000	1.133888000
H	3.111182000	1.353908000	1.455425000
H	2.824904000	-0.244077000	0.541632000
H	-0.137763000	1.975788000	2.508395000
H	1.387472000	2.770132000	2.060188000
H	0.021675000	2.756530000	0.935722000

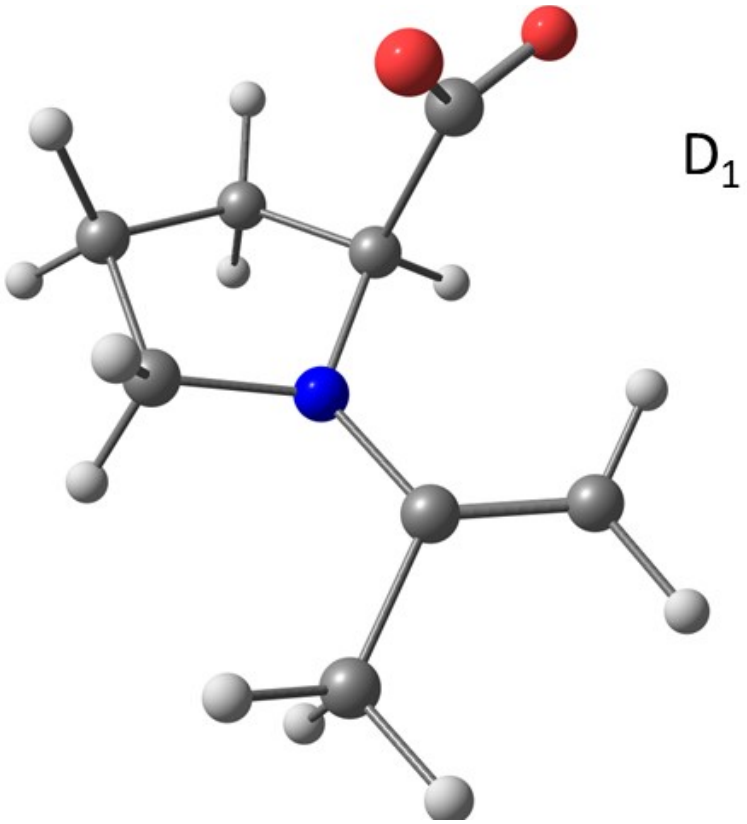

C	-1.864362000	-0.933602000	-0.323742000
C	-1.182598000	0.390261000	0.120591000
N	0.126696000	-0.003933000	0.637936000
C	0.504217000	-1.317905000	0.097721000
C	-0.857486000	-2.027323000	0.073160000
C	1.203096000	-1.366986000	-1.323398000
O	1.981343000	-2.356464000	-1.470361000
O	0.908269000	-0.473947000	-2.161297000
C	1.098700000	0.954533000	1.017370000
C	2.434452000	0.605418000	1.212549000
C	0.532488000	2.173902000	1.681649000
H	-2.818617000	-1.068573000	0.281600000
H	-2.056807000	-0.932407000	-1.402472000
H	-1.101686000	1.092326000	-0.731964000
H	-1.794986000	0.842567000	0.929971000
H	1.182703000	-1.804616000	0.817211000
H	-0.866328000	-2.905622000	-0.588138000
H	-1.142264000	-2.338104000	1.122561000
H	3.123983000	1.362987000	1.584238000
H	2.869266000	-0.262213000	0.732023000
H	0.053721000	1.961112000	2.695474000
H	1.317474000	2.924509000	1.842328000
H	-0.264912000	2.650673000	1.099217000

References

1 J. Kimling, M. Maier, B. Okenve, V. Kotaidis, H. Ballot and A. Plech, *J. Phys. Chem. B*, 2006, **110**, 15700–15707.

2 L. Cheng, K. Zhao, Q. Zhang, Y. Li, Q. Zhai, J. Chen and Y. Lou, *Inorg. Chem.*, 2020, **59**, 7991–8001.

3 F. Ishikawa, T. Tsumuraya and I. Fujii, *J. Am. Chem. Soc.*, 2009, **131**, 456–457.

4 E. Shah and H. P. Soni, *RSC Adv.*, 2013, **3**, 17453–17461.

5 C. L. Luu, T. T. V. Nguyen, T. Nguyen and T. C. Hoang, *Adv. Nat. Sci: Nanosci. Nanotechnol.*, 2015, **6**, 025004.

6 M. E. Casida, Recent advances in Density Functional Theory, World Scientific, Singapore 1995, **1**, 155–192.

7 C. Lee, W.Yang, R. G. Parr, *Phys. Rev. B,* 1988, **37 (2)**, 785–789.

8 R.Ahlrichs, M. Bär, M. Häser, H. Horn, C. Kölmel, *Chem. Phys. Lett.,* 1989, **162 (3)**, 165–169.